Chapter 7. Comparison of measured compressional wave properties to Biot Theory

In *Chapter 6* the validity of non-dispersive velocities and attenuation coefficients which are proportional to frequency were statistically confirmed within 95 % confidence limits for the majority of locations examined. However, it is useful to compare the measured properties to those predicted by Biot Theory for the fast compressional wave (*Section 2.5.2*), as this is the standard accepted geoacousic model utilised for marine sediment (*Section 2.5.2*). This project examines the original version of Biot Theory (Biot, 1956b; Biot, 1956a), which incorporates energy losses from global viscous mechanisms only, using a programme scripted by A. Best, *e.g.* see (Best *et al.*, 2001). The modified versions of Biot Theory, *i.e.* Biot-Stoll Theory and EGM, are omitted due to the lack of shear wave information for the inter-tidal sediments examined and the inability to obtain the complex shear moduli required for these models. For the purposes of clarity the phase velocities, attenuation coefficients and quality factors predicted by Biot Theory will be termed the Biot velocities, the absorption coefficients and the Biot quality factors respectively.

Biot Theory depends on eleven geotechnical properties of the sediment, which have been divided into pore fluid properties, mineral grains properties and sediment frame properties, *Section 2.5.2.* A number of authors misuse Biot theory, through the use of values of input properties, which are inapplicable to the sediment under examination, to produce optimum fits between measured and predicted properties (Richardson *et al.*, 2002). In addition the interrelated nature of certain parameters is often neglected, resulting in combinations of input parameters which are not relevant (Best, 1992; Stoll, 1979; Williams *et al.*, 2002). For example the porosity and grain size distribution will influence the pore size parameter, permeability, tortuosity and the bulk and shear moduli of the sediment frame. Coarser, less porous materials will possess a more tortuous, permeable structure with larger pores and increased bulk and shear moduli. Hence if the porosity input into Biot Theory is adjusted the values of the other frame properties should be suitably modified. The manner in which this project incorporates the interrelated nature of the above groups of geotechnical properties is described in *Section 7.1.*

7.1. Computing/measuring input parameters of Biot model

In order to incorporate the variability observed between different locations at the same general site (*Section 6.1.1* and *6.1.2*) the range of geotechnical properties obtained at each site will be used to obtain predicted compressional wave properties for each site only. The procedure followed within this study is to obtain an acceptable range of values of each input variable from either measured geotechnical properties, values in the literature or empirical/theoretical relationships. The inter-related manner of certain parameters are considered and the maximum and minimum limits of Biot velocity, absorption coefficient and Biot quality factor computed for each site. Mean input parameters for each site were also used to compute mean predicted values.

The manner in which the fluid properties, grain properties and sediment frame properties were obtained are detailed in *Sections 7.1.1, 7.1.2* and *7.1.3* respectively.

7.1.1. Calculating fluid properties

The fluid properties were derived from the measured salinity S and temperature T of the pore water, *Table 7.1,* using accepted empirical relationships, outlined in *Appendix A.* The resulting range of densities ρ_f, bulk moduli K_f and viscosities η_f for the sands and silts examined are displayed in *Table 7.1.*

Sediment	Salinity S (‰)	Temperature T (^oC)	Density ρ_f (kg·m^{-3})	Bulk modulus K_f (GPa)	Viscosity η_f (mPa·s)
Sand	0.3 – 6.3	14 – 18	999 – 1003	2.26 – 2.29	1.05 – 1.17
Silt	0.3 – 4.1	2.5 – 14.5	1000 – 1002	2.26 – 2.28	1.16 – 1.65

Table 7.1. Properties of pore water at sand and silt sites examined.

It is important to observe how the computed values compare to the range used in previous literature, *Table 2.4*. The densities obtained possess a maximum range of 4 kg·m^{-3} and correspond to the lowest densities used by previous researchers, *i.e.* 1000 to 1030 kg·m^{-3}. This is a result of the density of seawater being dominated by salinity, rather than temperature, and the selected fieldsites being located in estuarine and inter-tidal environments. Fluid bulk densities lie within the range observed in the literature, *i.e.* 2 to

2.42 GPa. For sand sites, fluid viscosities lie approximately within the previously published range of 0.95 to 1.15 mPa·s, while fluid viscosities for silts sites exceed this range. This may be a consequence of the temperatures at the silt sites lying below the range of temperatures for which the empirical relationships used to obtain fluid viscosity are valid, *Appendix A.* As fluid viscosity is expected to have negligible effect on the compressional wave properties predicted by Biot Theory (Hovem and Ingram, 1979; Williams *et al.*, 2002), the values in *Table 7.1* are retained.

The fluid properties are inter-related, through their dependence on temperature and salinity. Maximum densities, bulk moduli and viscosities all correspond to minimum salinities and maximum temperatures, with effects of temperature change on density being negligible to an accuracy of 1 $kg \cdot m^{-3}$.

7.1.2 Estimating grain properties

The range of grain densities and bulk moduli were obtained from the literature, *Table 2.4*. The range of grain densities used originates from sediment samples in the upper 0.3 m of the sediment column and a wide range of environments, with the majority of values lying between 2650 and 2750 $kg \cdot m^{-3}$ (Hamilton and Bachman, 1982). The choice of mineral bulk moduli values has been more selective, due to the dependence of the bulk moduli on the measurement technique. Bulk moduli measured under high stress and strain conditions will be lower than the dynamic values required for acoustic modelling purposes, due to the relatively small stresses and strain applied by acoustic waves (Richardson *et al.*, 2002). Hence the selected range of 32 to 49 GPa incorporates values of mineral bulk moduli which have been previously used in the application of geoacoustic models to marine sediments. For modelling purposes, the mineral densities and bulk moduli are assumed to be unrelated. In the absence of a detailed examination of the mineral composition of the sediment samples, the use of values from literature is justified.

7.1.3. Measuring and calculating sediment frame properties

The remaining geotechnical parameters required are all connected to the sediment frame, and are hence intrinsically interrelated. The approach used was to obtain maximum, minimum and mean values of porosity and mean grain diameter for each site, with values corresponding to the corrupted locations of Lilliput 2, Mercury 1 and Mercury 3 omitted,

see *Sections 6.1.1* and *6.1.2.* The maximum and minimum values are considered to be an accurate assessment of the variability at each site. Valid ranges of additional frame parameters *i.e.* bulk and shear moduli, permeability, pore size and tortuosity, were computed from these porosities and mean grain diameters and are displayed in *Table 7.2.* The retention of only one uncorrupted location at the Mercury site allowed only mean values of porosity and mean grain diameter to be obtained. The interrelated nature of the properties restrict the manner in which the properties which can be combined, *i.e.* the maximum value of porosity can only be used along with the minimum values of shear modulus, bulk modulus and structure parameter and maximum values of pore size parameter and permeability. The over-estimation of *in situ* porosities by the measurement techniques adopted (see *Appendix C*) will result in a corresponding under-estimate of frame bulk modulus, shear modulus and tortuosity and over-estimate of pore size parameter and permeability, the consequences of which are discussed in *Section 6.2.* The manner in which the additional frame properties were computed from porosity and mean grain diameter is detailed below.

Range of values	Sites					
	Studland	Branksome	Lilliput	Needs Ore	Saltern	Universe
n (%)	39.1 - 55.3	40.2 - 40.3	42.6 - 50.7	82.0 - 91.9	92.5 - 92.7	75.9 - 90.2
M (μm)	259.4 - 423.3	255.1 - 307.7	206.3 - 225.6	4.2 - 10.5	8.4 - 10.0	13.0 - 13.4
K_b (GPa)	0.227 - 1.112	0.988 - 0.998	0.339 - 0.789	0.006 - 0.018	0.006	0.008 - 0.032
μ (MPa)	4.1 - 108.0	17.2 - 97.4	6.6 - 76.2	0.1 - 1.4	0.1 - 0.6	0.8 - 3.1
k ($10^{-11}m^2$)	5.90 - 84.30	4.97 - 9.66	5.53 - 15.08	0.08 - 7.24	2.78 - 4.12	0.35 - 3.81
a (μm)	55.4 174.6	59.2 69.3	50.9 78.8	6.4 40.1	34.6 42.1	13.7 41.2
γ	1.40 - 1.78	1.74	1.48 - 1.67	1.04 - 1.11	1.04	1.05 - 1.16

Table 7.2. Ranges of input properties which depend on the sediment frame, including porosity n, frame bulk modulus K_b, shear modulus μ, permeability k, pore size parameter a and structure constant γ. Mean grain diameter M is required for the calculation of permeability and pore size parameter.

- **Shear modulus and frame bulk moduli**

Shear modulus μ and bulk modulus K_b are related through

$$\mu = \frac{3K_b(1-2\sigma)}{2(1+2\sigma)} \qquad 7.1,$$

where σ is Poisson's ratio (Ogushwitz, 1985a). For surficial marine sediment Poisson's ratio varies from 0.453 to 0.491 (Hamilton, 1971a).

Hence bulk and shear moduli can be computed through the use of empirical relations to obtain either shear or bulk modulus from porosity and the use of *Equation 7.1* to compute the other modulus (Ogushwitz, 1985a). An examination of the literature displays the limited porosity range spanned by empirical relations which relate shear

modulus to porosity, *i.e.* 33 to 60 % (Hardin and Black, 1968; Hardin and Richart, 1963), 26 to 71 % (Bryan and Stoll, 1988) and 66 to 91 % (Lu *et al.*, 1998b). In addition empirical relationships for silts and clays possess considerably different forms (Bryan and Stoll, 1988; Lu *et al.*, 1998b). More reliable and consistant empirical relationships between bulk modulus, in units of GPa, and fractional porosity have been derived by (Hamilton, 1971a) for both natural sands

$$K_b = 10^{(1.70932 - 0.0425391 \cdot n)} \qquad 7.2a,$$

and natural silt-clays

$$K_b = 10^{(1.7358 - 0.0425075 \cdot n)} \qquad 7.2b.$$

These have been derived from acoustical measurements of surficial sediments and are directly applicable to this project. Though separate equations are required for sands and silt-clays, the porosity range of which are undefined, the similarity of the two equations to the general relationship for porosities from 0 to 90 %, highlights the consistency and reliability of these relationships.

Hence the approach adopted is to estimate the range of frame bulk modulus applicable to each site, from the range of porosities and either *Equation 7.2a* or *7.2b.* The range of shear modulus values was then calculated from *Equation 7.1* using values of Poission's ratio from 0.453 to 0.491.

The resulting ranges of bulk moduli, *Table 7.2,* agree well with those observed in the literature (*Table 2.4, Section 2.5.2).* Bulk moduli for sands range from 0.027 to 1.112 GPa and lie within the upper end of the published range, while values for silts range from 0.006 to 0.032 GPa, which extends slightly below the published range.

- **Pore size**

The pore size was computed from the hydraulic radius *HR*, which is the ratio of the volume filled with fluid to the wetted surface area. For a medium consisting of uniform spherical grains of diameter M this is calculated from

$$HR = \frac{M}{6} \frac{0.01 \cdot n}{(1 - 0.01 \cdot n)} \qquad 7.3.$$

The pore size radius used by Biot (1956b) can be replaced by the pore size parameter *a* (Hovem and Ingram, 1979), which is given by

$$a = 2 \cdot HR = \frac{M}{3} \frac{0.01 \cdot n}{(1 - 0.01 \cdot n)} \qquad 7.4.$$

Hence the pore size parameter incorporates both the size of the grains and the more open structure of high porosity sediments.

The resulting pore size parameters computed for each site, *Table 7.2,* range from 50.9 to 174.6 μm in sands and 6.4 to 42.1 μm in silts. Though these agree well with the published range of 0.1 to 39 μm (*Table 2.4, Section 2.5.2*) for silts, the values for sands are greater than expected. However, the use of *Equation 7.3* to successfully predict the velocity and attenuation coefficient for range of marine sediments, which contain non-spherical particles with a range of grain diameters, confirms its applicability (Hovem, 1980; Hovem and Ingram, 1979; Ogushwitz, 1985a; Ogushwitz, 1985b). The differences between the calculated values in *Table 7.2* and the published range of values are attributed to the scarcity of pore-size measurements in marine sediments.

- **Permeability**

Permeability k was computed from the Kozeny-Carman Equation

$$k = \frac{n \cdot HR^2}{k_o} = \frac{(0.01 \cdot n)^3}{(1 - 0.01 \cdot n)^2} \frac{M^2}{36 k_o} \qquad 7.5,$$

where k_o accounts for the tortuosity and shape of the pores. For spherical uniform sized grains k_o is approximately 5, with this value confirmed for sands (Hovem and Ingram, 1979). A value of 3 to 7 is observed for spherical, fibrous and flat-sided grains with porosities from 30 to 80 %, while k_o may exceed 10 for porosities greater than 80 % (Carman, 1937). The Kozeny-Carman equation has been used to successfully fit Biot predictions of velocity and attenuation coefficient to measured values for sands and glass beads, with a porosity of 36 % (Hovem and Ingram, 1979) and mixtures of clay and fine sand particles with porosities from 62 to 98 % (Ogushwitz, 1985b). These authors use values for k_o of 5 and 3 to 10 respectively, and though the later authors examine the effect of k_o on predicted velocities and attenuation coefficients the results are inconclusive.

Hence the permeability range for each site is computed from the Kozeny-Carman Equation, using a value of k_o of 5 for sand sites and 10 for silt sites, *Table 7.2.* For the silt sites the resulting permeabilities fall within the observed range in the literature ($2.5 \cdot 10^{-14}$ to $6.1 \cdot 10^{-11}$ m^2 from *Table 2.4)*. Permeability ranges at the Lilliput and Branksome sites

broadly agree with the upper limit of published values, while the range of permeabilities at the Studland site is much greater than those previously observed. Confidence in the Kozeny-Carmen Equation justifies the use of such values.

- **Tortuosity**

  Tortuosity γ is computed from porosity using

$$\gamma = 1 - \gamma_o\left(1 - \frac{1}{0.01 \cdot n}\right) \qquad 7.6,$$

where γ_o is derived from a microscopic model of the fluid moving in the frame (Berryman, 1980). Theoretically values γ_o of are limited to $0 \leq \gamma_o \leq 1$, with a value of 0.5 applicable to spherical particles. This relationship has been used by Ogushwitz (1985b) to predict the velocity and attenuation coefficient of suspensions of clay and sand particles with porosities from 62 to 98 %. Numerical calculations performed for face-centred cubic granular material also support *Equation 7.6,* though suggest a value of γ_o of 0.227 (Yavari and Bedford, 1991).

As broad support exists for the applicability of *Equation 7.6*, with a value of γ_o of 0.5, for natural sediments (Ogushwitz, 1985b), structure factors were computed using this approach. The resulting range of tortuosities varies from 1.4 to 1.78 in sands and 1.04 to 1.11 in silts. Though values for silts are less than the published range of 1.15 to 1.71, *Table 2.4*, the above supporting evidence for *Equation 7.6* and the fact that the silt values lie within the theoretical limits of 1 to 3 (Stoll, 1974) supports these new values.

7.2. Comparsion of Biot predictions to measured properties in sands and silts

The comparison of the measured velocities, attenuation coefficients and quality factors to the Biot velocities, absorption coefficients and Biot quality factors at each site is displayed in *Figures 7.*1 to *7.7*. In order to allow frequency-dependent variations to be clearly observed the mean values of Biot velocity, absorption coefficient and Biot quality factor are plotted independently for all sites. In the case of the Mercury site the retention of only one uncorrupted location permits the calculation of mean Biot properties only.

The phase velocities predicted by Biot Theory for the sand sites generally agree with the measured group velocities, with Biot velocities ranging from 1600 to 1820 $m \cdot s^{-1}$ (*Figures 7.1A, 7.2A* and *7.3A*). Some exceptions occur, with Biot velocities exceeding

measured velocities for all frequencies at Branksome 1 (*Figure 7.2A*) and frequencies less than 50 kHz at Lilliput 1 *(Figure 7.3A*). At Branksome 1 this may be explained by disrupted received signals at frequencies of 60 kHz and less, owing to considerable electronic noise, *Appendix D,* with the majority of measured velocities at frequencies greater than 60 kHz agreeing with Biot velocities within errors.

Biot velocities ranged from 1440 to 1500 $m \cdot s^{-1}$ in silts and are generally greater than those measured (*Figures 7.4A, 7.5A, 7.6A* and *7.7A*), with agreement between the two velocities only observed for Needs Ore 3 (*Figure 7.4A*). The Biot velocities were typically greater than the velocity of pore water (1420 to 1476 $m \cdot s^{-1}$, *Section 6.1.1*). As the velocities agree for sands, and the wave-shape of received signals in silts and sands were observed to be similar, *Section* 5.2.2, the discrepancy between predicted and observed velocities in silts cannot be attributed to the measurement of a group velocity by the *in situ* experiments and the prediction of a phase velocity by Biot theory. Assuming that the geotechnical measurement techniques adopted in this project over-predicted porosity by as much as 20 % (see comparison of measured porosities to those from literature in *Table 4.5, Section 4.4.3*), Biot velocities were recomputed. This decrease in porosity produced a corresponding decrease in velocity less than 20 $m \cdot s^{-1}$, and hence the discrepancies between measured and *in situ* porosities cannot be used to explain the difference between the measured velocities and those predicted by Biot Theory.

Alternative explanations are either that the measured velocities in silts are suspect or that the bulk moduli used for the silts are too great. This can occur either though:

- A reduction in the composite grain bulk modulus, owing to the presence of a significant proportion of organic matter (see *Section 6.1.2*).
- Or the frame bulk moduli calculated from *Equation 7.1* being too great for the inter-tidal silts examined. This may arise from differences between the framework of inter-tidal sediments and submerged sediments. As the empirical equations relate frame bulk moduli to porosity, such variations include differences in the sorting, modality and dominant grain diameters of the sediment distribution, all of which will affect the number of grain-to-grain contacts and the frame bulk moduli.

The mean Biot velocities predict dispersions of less than 0.5 % in sands and 1.5 % in silts, over the frequency range of 16 to 97 kHz, *i.e.* a difference of less than 12 $m \cdot s^{-1}$ in sands and 22 $m \cdot s^{-1}$ in silts. It is highly unlikely that these relatively small differences in

velocity will be distinguishable within the errors in velocities ($\pm$ 20 to $\pm$ 70 $m \cdot s^{-1}$ in sands and less than $\pm$ 25 $m \cdot s^{-1}$ in silts, *Sections 6.2.1* and *6.2.2*) and the spread of velocity values. This spread arises from both the non-unique nature of sediment (*Section 2.4.1*) and the observation of varying degree of sediment heterogeneity at the locations examined, with the sediment variability ΔM ranging from 1.9 to 19.8 % (*Section 4.4.3*) and larger heterogeneities, such as shells, pebbles, root material and possible biogenic burrows observed at several locations (*Appendix B*).

In sands, values of absorption coefficient range from approximately 1 to 10 $dB \cdot m^{-1}$, with a maximum range of 3 $dB \cdot m^{-1}$ existing at a single frequency and site (*Figures 7.1C, 7.2C* and *7.3C*). Conversely, the measured attenuation coefficients display much larger values, up to 52 $dB \cdot m^{-1}$, and much larger variations, with a maximum range of 24 $dB \cdot m^{-1}$ at the same frequency and site. The discrepancies between the measured attenuation coefficient and the absorption coefficient are attributed to additional loss mechanisms which are omitted by Biot Theory. For saturated marine sediments, feasible additional loss mechanisms include squirt flow and scattering losses, as both these mechanisms will account for the increased discrepancy at higher frequencies (Cascante, 1996). However, in order to determine which loss mechanisms is more valid, the application of both a scattering model and Biot-Stoll Theory would be required, the examination of which is beyond the scope of this thesis.

An additional point of debate is whether the additional losses arise from individual grains or larger heterogeneities. For the case of scattering, it is unlikely that Rayleigh scattering from sediment grains is a significant source of energy loss, owing to the wavelength corresponding to the highest received frequency (16 mm) being much greater than the diameters of the grains present (less than 1mm). This is supported by the observation that Rayleigh scattering is only significant for frequencies greater than 500 kHz in sands with a mean grain diameter of 1.27 phi (Williams *et al.*, 2002), which are coarser than all locations examined within this project, barr Studland 1. The sediment samples examined from the sand sites displayed evidence for larger scattering centres, *i.e.* slate fragments at the Branksome site with diameters up to 5 mm and pebbles and shells at the Studland site with diameters up to 15 cm. The existence of root material at the Lilliput site provides possible scattering centres and a mechanism through which channels can be produced, which may act as additional scattering centres. In addition, patches of sediment

with slightly different grain size distributions can act as scattering centres (*Section 4.4.3*). Under-estimations of observed attenuation coefficients by Biot Theory has been reported by previous authors, whom attribute the additional energy losses to scatter from clusters of sediment grains (Gorgas *et al.*, 2002), scatter from larger particles (Gorgas *et al.*, 2002; Williams *et al.*, 2002) or additional squirt flow from patches of sediment heterogeneity (Best *et al.*, 2001). At lower frequencies of 16 kHz the attenuation coefficients and absorption coefficients agree for Branksome 2 and Lilliput 4, implying global viscous losses can account for energy losses better at these frequencies.

In silts, the relationship between absorption coefficient and the measured attenuation coefficient is more variable, with predicted absorption coefficients varying from 1 to 50 $dB \cdot m^{-1}$. Though these values are relatively large, they lie within the range previously predicted by Biot Theory for typical silts and sands, *i.e.* 0.5 to 9 $dB \cdot m^{-1}$ at 16 kHz to 6 to 80 $dB \cdot m^{-1}$ at 97 kHz (Stoll and Bautista, 1998). For Needs Ore, measured and predicted values agree for frequencies from 16 to 35 kHz, while predicted values exceed those measured at higher frequencies (*Figure 7.4C*). At the Mercury and Saltern sites, absorption coefficients are greater than measured attenuation coefficients (*Figures 7.5C* and *7.7C* respectively). The absorption coefficients agree with measured attenuation coefficients from 40 to 65 kHz at Universe 1, and exceed measured values for other frequencies at Universe 1 and all frequencies at Universe 2 (*Figure 7.6C*). Hence for the majority of silt sites examined the absorption coefficient predicted by Biot Theory is greater than the attenuation coefficient measured.

The discrepancy between the measured attenuation coefficients and absorption coefficients predicted by Biot Theory can be explained through the over-estimation of *in situ* porosities by the geotechnical measurement techniques adopted (see *Appendix* C). An over-estimate of porosity will produce over-estimates of permeability and pore size parameter and under-estimates of tortuosity, all of which act to increase the predicted absorption coefficient. As porosity, permeability, pore size parameter and tortuosity represent four of the six factors which have a "significant" effect on absorption coefficients (see *Table 2.7, Section 2.5.2*) predictions of absorption coefficient will be considerably over-estimated.

From 16 to 97 kHz, the mean absorption coefficients depend on $f^{1/2}$ in sands and f^{2} in silts. It is difficult to visibly distinguish between the underlying quadratic relationship

and a linear relationship for silts. This highlights the difficulty in distinguishing between linear and non-linear relationships for frequency ranges which span a frequency range of a decade or less (Kibblewhite, 1989).

Measured quality factors are much less than those predicted in sands, a result of the observed discrepancy between measured attenuation coefficients and predicted absorption coefficients, which has been primarily attributed to significance of scattering losses. In silts the measured and predicted values of quality factor agree at the following frequencies: greater than 65 kHz at the Saltern site; less than 65 kHz at Universe 1; between 29 and 45 kHz at Mercury 2 and less than 35 kHz at Needs Ore 1 and 2. Outside these ranges Biot quality factors are generally less than the measured quality factors. This simply restates the tendency of the Biot Theory implemented to over-predict attenuation coefficient in the silts examined. Biot quality factors increase with $f^{1/2}$ for sands (*Figures 7.1E., 7.2E* and *7.3E*) and vary with f^{1} in silts (*Figures 7.4E, 7.5E, 7.6E*) and *8.7.E.* These simply reflect the dependence of absorption coefficient on $f^{1/2}$ in sands and f^{2} in silts and the relationship between quality factor and attenuation/absorption coefficient, *Equation 2.8.* The inability of earlier statistical analysis to determine a reliable relationship between quality factor and frequency, *Sections 6.1.1* and *6.1.2,* combines with the large discrepancies between the predicted and measured values to prevent any conclusions being drawn concerning the frequency-dependence of quality factor in inter-tidal sediments.

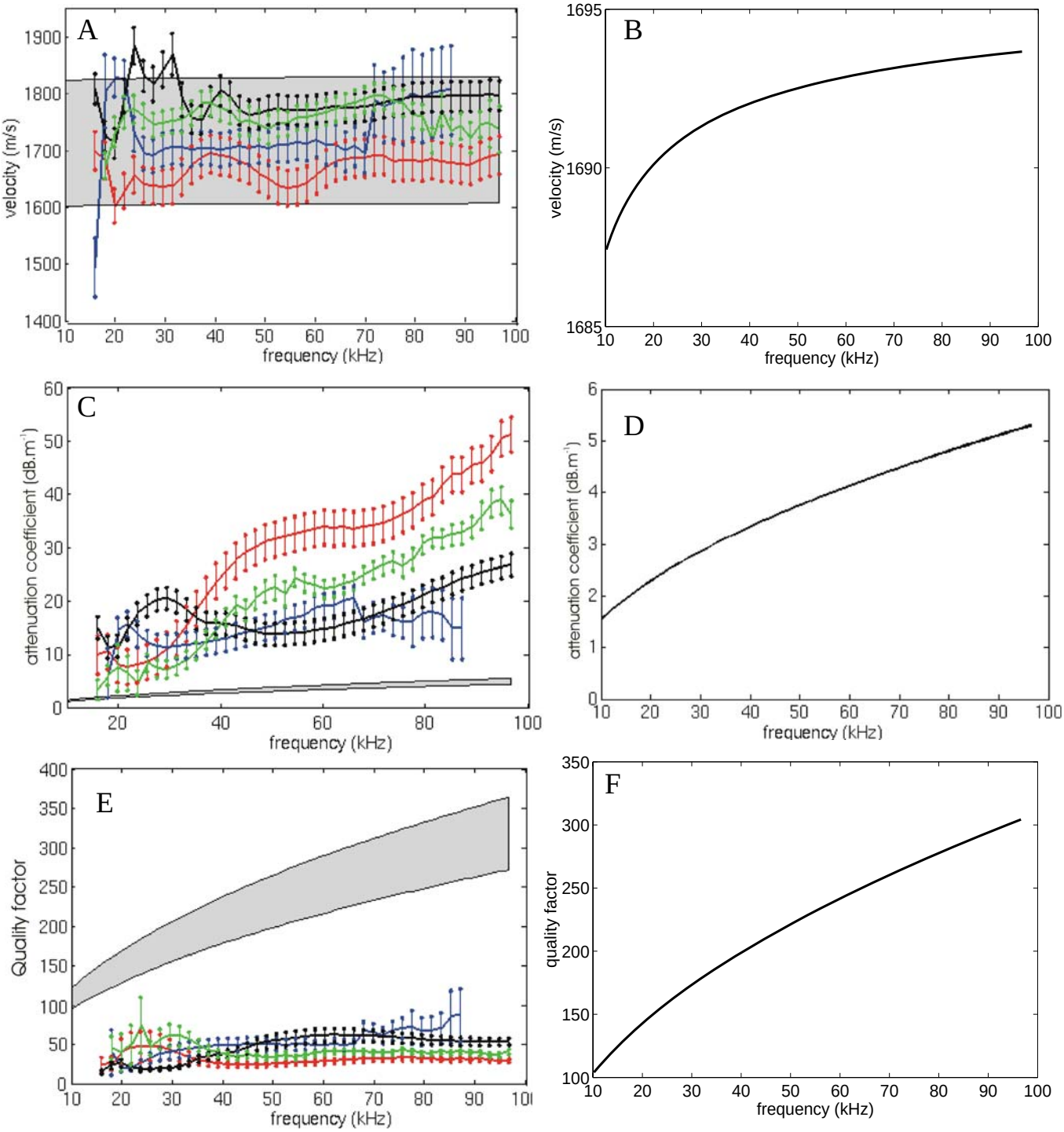

Figure 7.1. Comparison of measured compressional wave properties observed at the Studland site to the Biot velocity (A), absorption coefficient (C) and Biot quality factor (E). Measured properties are plotted for Locations 1 (red), 2 (blue), 3 (black) and 4 (green), along with the range of Biot predictions (shaded area) and the mean values of Biot velocity (B), absorption coefficient (D) and Biot quality factor (F).

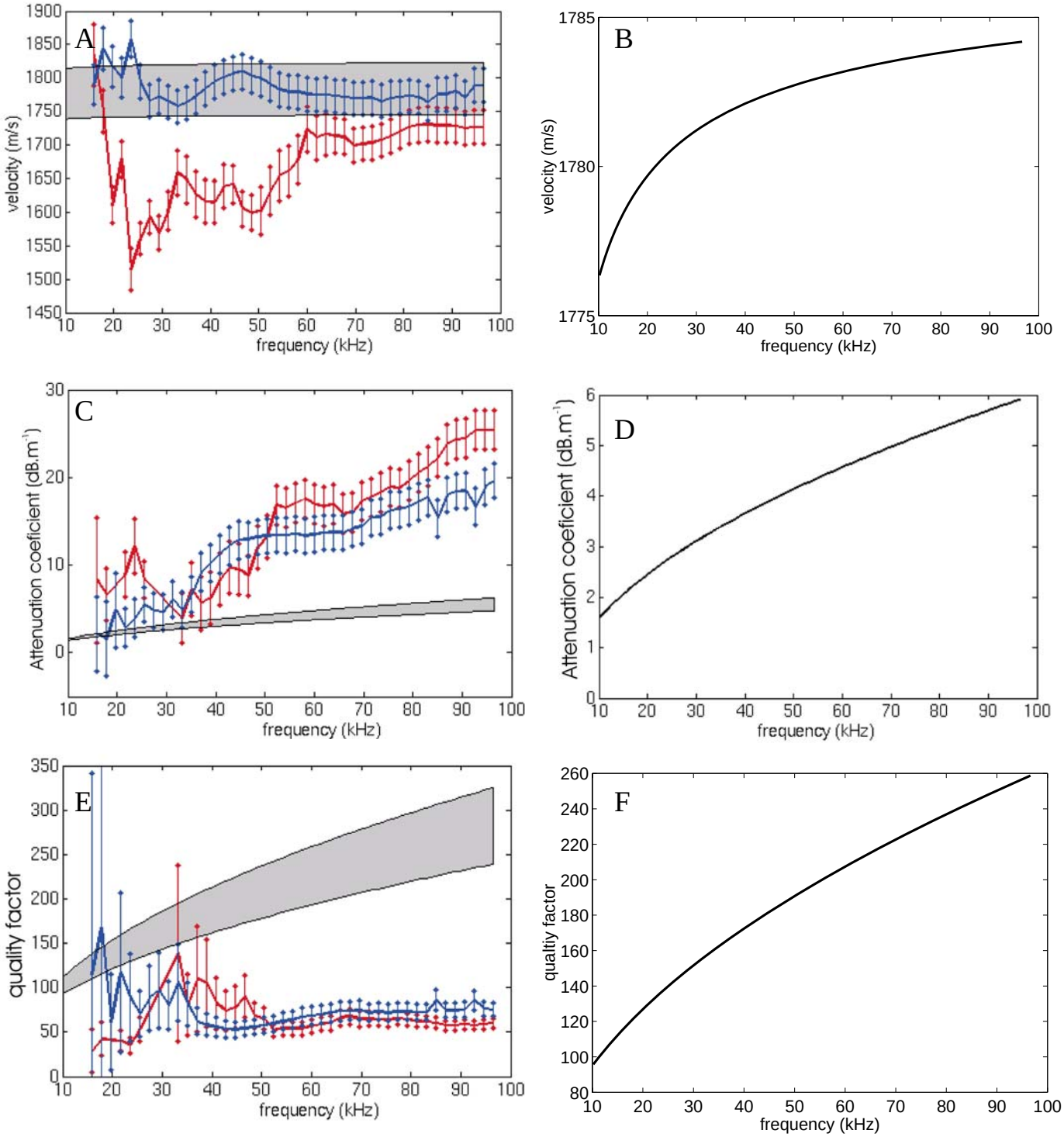

Figure 7.2. Comparison of measured compressional wave properties observed at the Branksome site to the Biot velocity (A), absorption coefficient (C) and Biot quality factor (E). Measured properties are plotted for Locations 1 (red) and 2 (blue), along with the range of Biot predictions (shaded area) and the mean values of Biot velocity (B), absorption coefficient (D) and Biot quality factor (F).

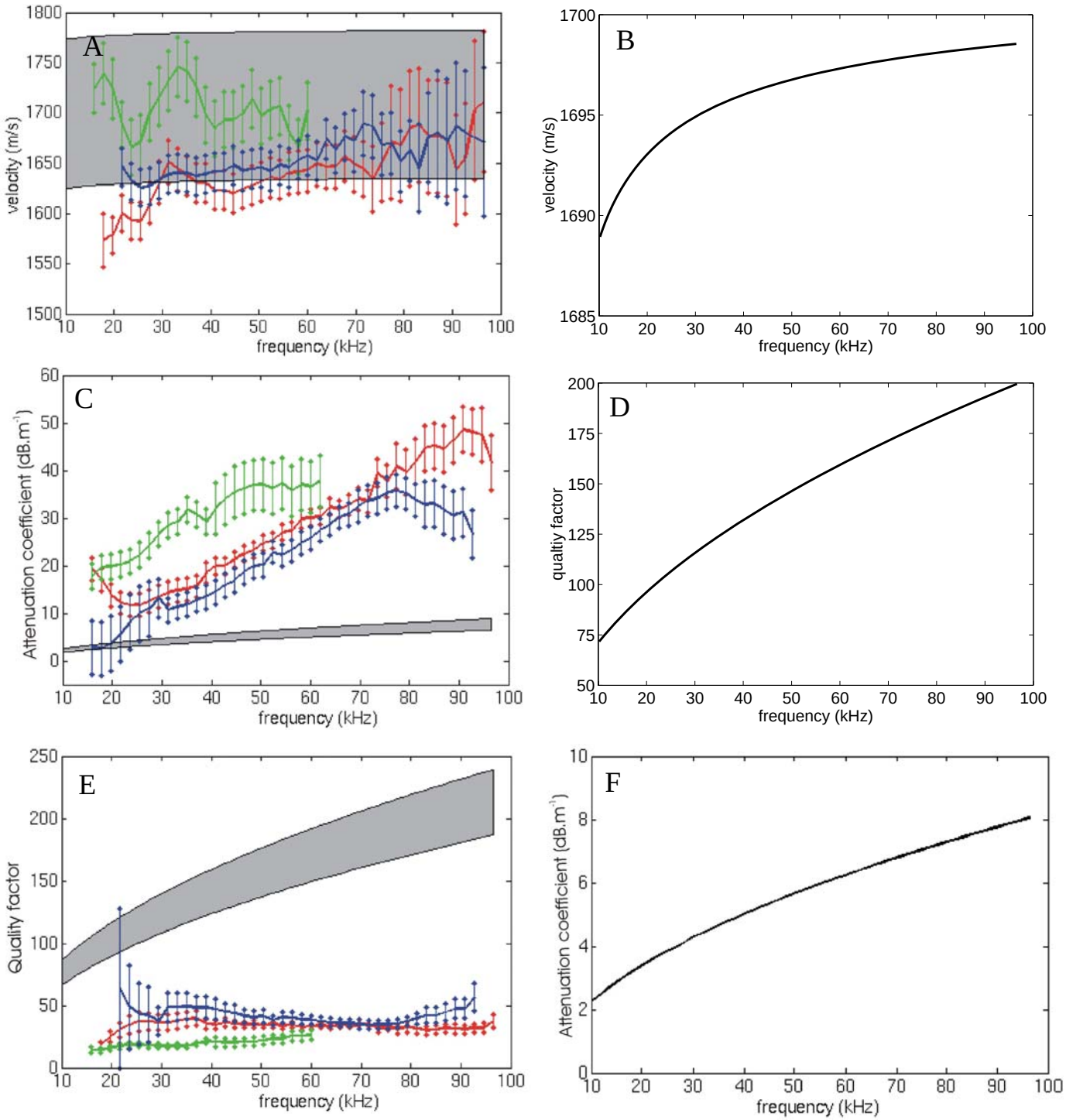

Figure 7.3. Comparison of measured compressional wave properties observed at the Lilliput site to the Biot velocity (A), absorption coefficient (C) and Biot quality factor (E). Measured properties are plotted for Locations 1 (red), 3 (green) and 4 (blue), along with the range of Biot predictions (shaded area) and the mean values of Biot velocity (B), absorption coefficient (D) and Biot quality factor (F).

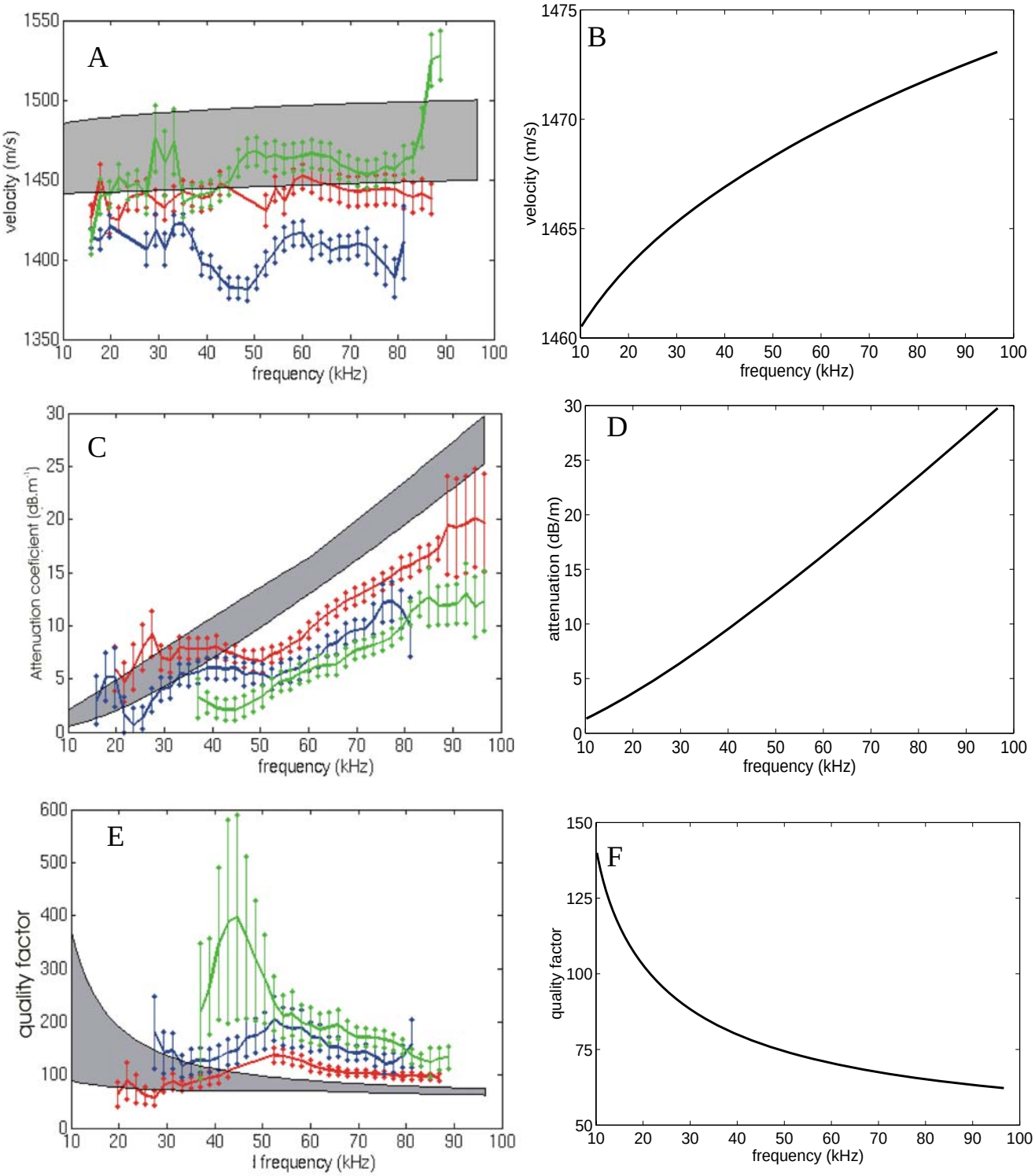

Figure 7.4. Comparison of measured compressional wave properties observed at the Needs Ore site to the Biot velocity (A), absorption coefficient (C) and Biot quality factor (E). Measured properties are plotted for Locations 1 (red), 2 (green) and 3 (blue), along with the range of Biot predictions (shaded area) and the mean values of Biot velocity (B), absorption coefficient (D) and Biot quality factor (F).

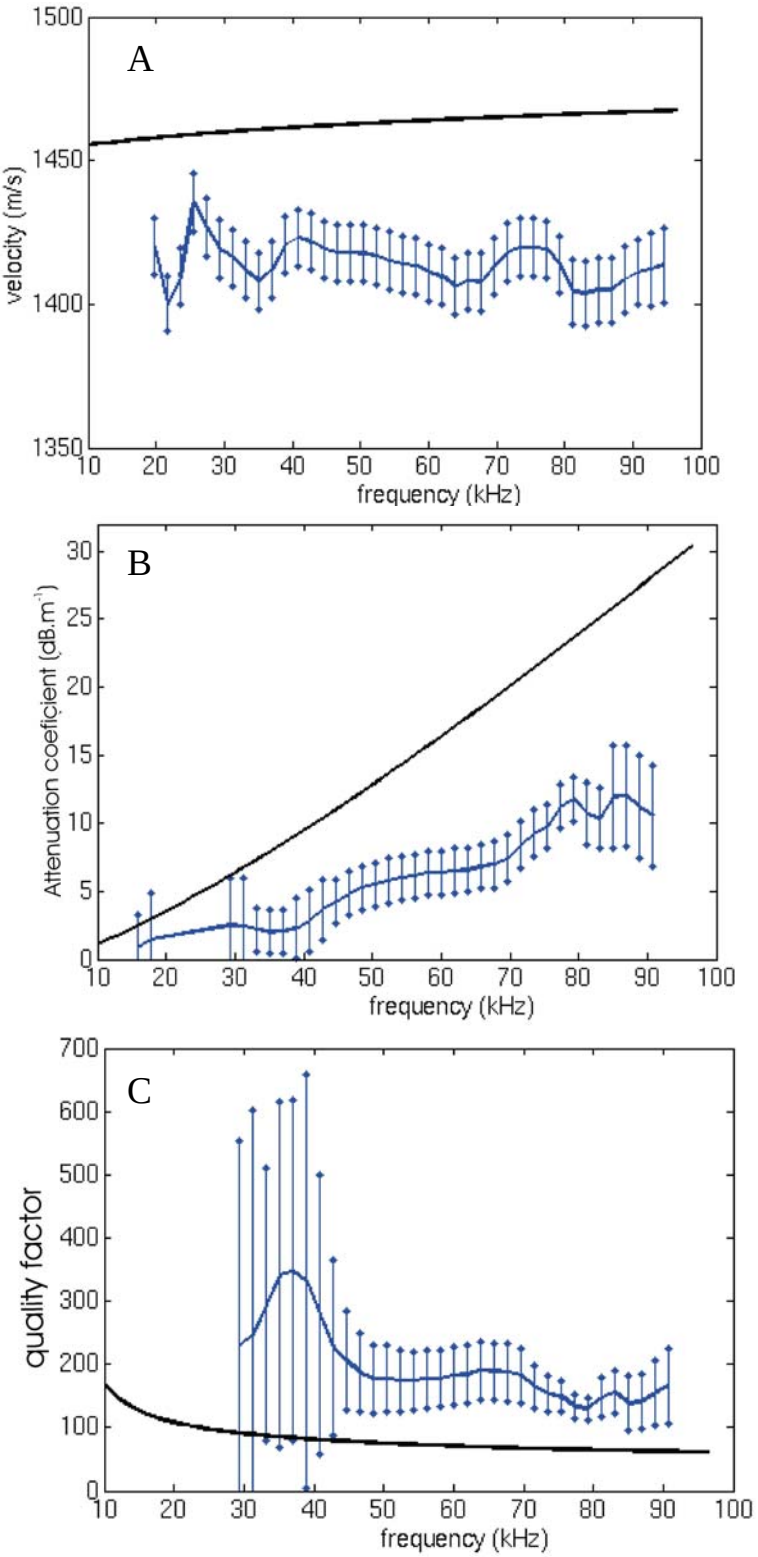

Figure 7.5. Comparison of measured compressional wave properties observed at Mercury 2 (blue) to those predicted by Biot Theory (black line), including velocities (A), attenuation/absorption coefficients (B) and quality factors (C).

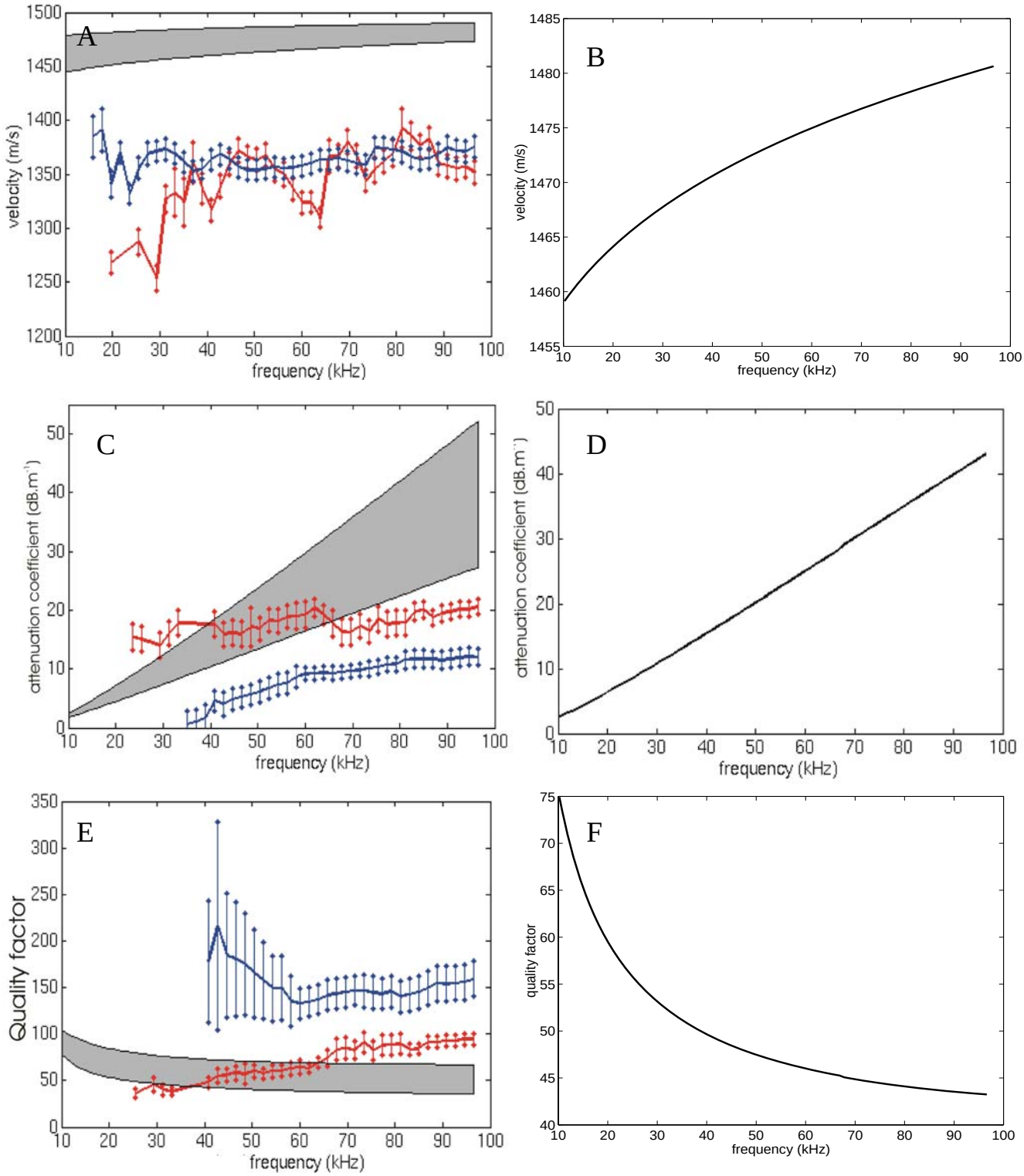

Figure 7.6. Comparison of measured compressional wave properties observed at the Universe site to the Biot velocity (A), absorption coefficient (C) and Biot quality factor (E). Measured properties are plotted for Locations 1 (red) and 2 (blue), along with the range of Biot predictions (shaded area) and the mean values of Biot velocity (B), absorption coefficient (D) and Biot quality factor (F).

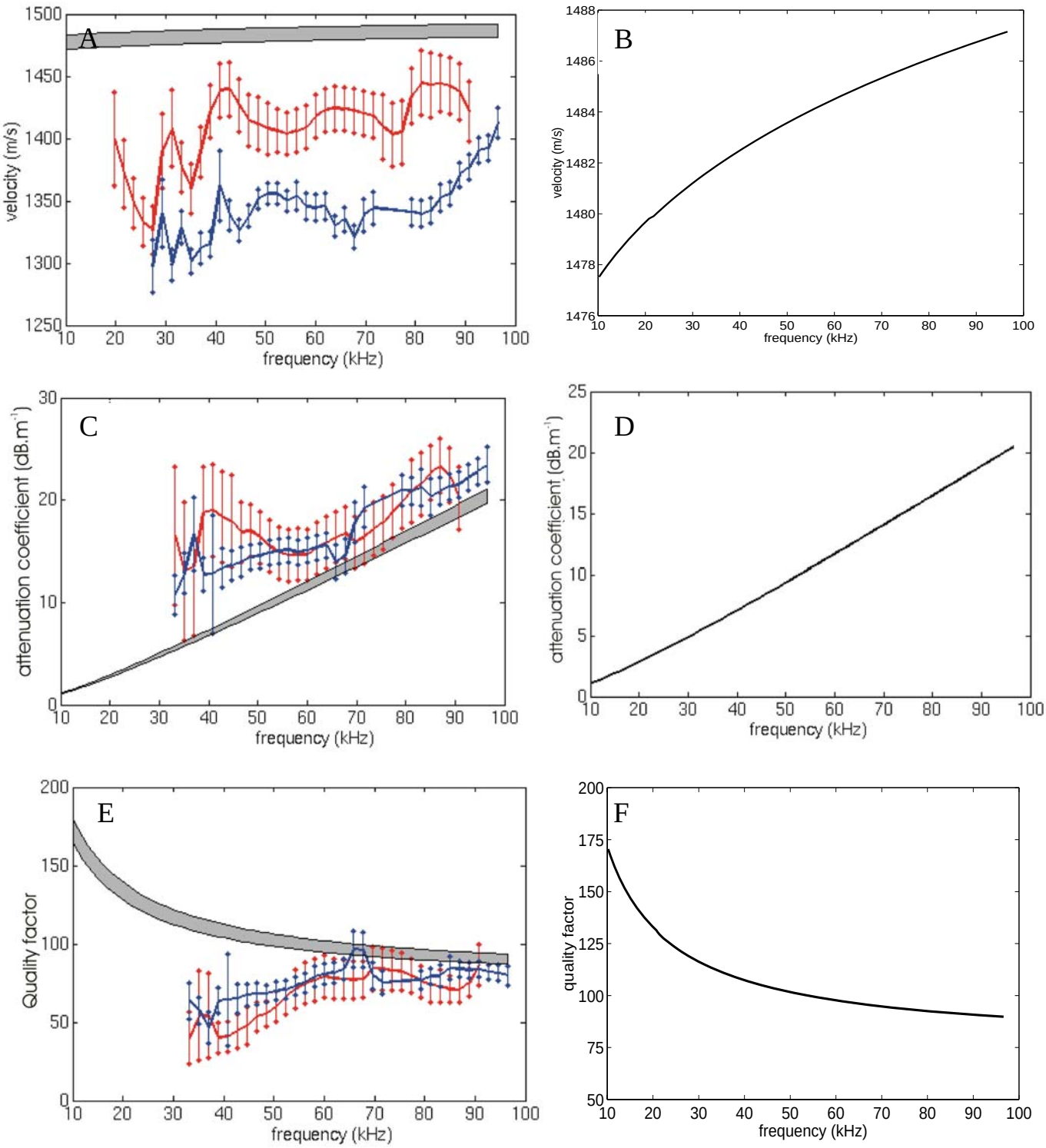

Figure 7.7. Comparison of measured compressional wave properties observed at the Saltern site to the Biot velocity (A), absorption coefficient (C) and Biot quality factor (E). Measured properties are plotted for Locations 1 (red) and 2 (blue), along with the range of Biot predictions (shaded area) and the mean values of Biot velocity (B), absorption coefficient (D) and Biot quality factor (F).

7.3. Summary

The original version of Biot Theory was used, implemented in such a manner that predicted compressional wave properties obtained are applicable to the sediment examined at each site. Fluid properties were based on measured salinities and temperatures of water and frame properties were obtained from the porosity and mean grain size of the sediment examined. Within each category of physical properties, *i.e.* those of the fluid, mineral grains and sediment frame, the interrelated nature of the properties was considered.

In sands, the velocities predicted by Biot Theory agree with those measured. Predicted absorption coefficients are less than measured attenuation coefficients in sands, with the discrepancy between predicted and measured values increasing with frequency. Either scattering or squirt flow are promoted as additional loss mechanisms, with no manner of distinguishing between them available. An additional issue is whether the increased losses occur from individual grains or sediment heterogeneities. In the case of scattering losses, larger scale heterogeneities observed within the sediment examined, *e.g.* shells, pebbles, root channels, rubble or patches of sediment heterogeneity, are the more likely cause of energy loss.

In silts, predicted velocities are greater than those measured, while absorption coefficients generally agree with or are greater than measured attenuation coefficients. The discrepancy between the measured attenuation coefficients and absorption coefficients predicted by Biot Theory can be explained through the over-estimation of *in situ* porosities by the geotechnical measurement techniques adopted (see *Appendix* C), which results in over-estimates of pore size parameter, permeability and under-estimates of tortuosity. The discrepancies between measured and *in situ* porosities cannot be used to explain the difference between the measured velocities and those predicted by Biot Theory. Hence, alternative explanations for the discrepancies in measured and predicted velocities are either that the measured velocities in silts are suspect or that the bulk moduli used for the silts are too great.

The levels of dispersion predicted by Biot Theory, *i.e.* <1.5 %, would not have been observable with the errors and spread of the measured velocities. Over the examined frequency range of 16 to 96 kHz it is impossible to distinguish between the complex frequency dependence predicted by Biot Theory and a linear relationship. Hence a

frequency range of greater than 1 decade is required to examine frequency dependence of attenuation coefficient. Predicted quality factors confirm the above conclusions drawn concerning the validity of Biot Theory and the energy loss mechanism present.